DISORDERED VORTEX FLOW COMPUTED AROUND A CRANKED DELTA WING AT SUBSONIC SPEED AND HIGH INCIDENCE

ICAS-86-1.4.1

Arthur Rizzi*
FFA, The Aeronautical Research Institute of Sweden, S-161 11 BROMMA, Sweden
and
Charles J. Purcell+
ETA Systems, Inc., St. Paul, MN 55113, U.S.A.

Abstract

A numerical method that solves the Euler equations for compressible flow is used to study leading-edge vortex dynamics. The particular cases simulated are subsonic flow M_∞=0.3 around a twisted and cambered cranked-and-cropped delta wing at two angles of attack, α=12.5 and 20 deg. This geometry induces multiple leading-edge vortices in a straining velocity field that brings about a spiralling flow instability.The discretization contains over 600,000 cells and offers sufficient degrees of freedom in the solution to exhibit the onset of chaotic vortex flow that could well lead to vortex bursting. These two cases are studied to observe the behaviour of the vortex at high incidence angles. The simulated results are compared with wind-tunnel measurements. The agreement at inboard sections is reasonable for the position and strength of the leading-edge vortex, but outboard it is poor because of the complex transition to disordered vortex flow at the tip. Both the numerical simulation and the experimental measurements show that the flow at α=12.5 deg. is unsteady. The computations predict a premature bursting of the vortex at α=20 deg. and the flow is again steady.

Nomenclature

C_L = lift coefficient
C_D = drag coefficient
$\vec{E}$ = rate-of-strain tensor
$\vec{e}_x, \vec{e}_y, \vec{e}_z$ = Cartesian unit vectors
FD = total flux differences
$\vec{H}(q) = q\vec{V} + p[0, \vec{e}_x, \vec{e}_y, \vec{e}_z]$ flux
M_∞ = freestream Mach number
$\vec{n}$ = unit normal vector
p = static pressure
p_t = total pressure
q = $[\rho, \rho u, \rho v, \rho w]$ variables
$\vec{V}$ = velocity vector
u,v,w = Cartesian components of $\vec{V}$
x,y,z = Cartesian coordinates
α = angle of attack
ρ = density
T = artificial viscosity model
$\vec{\omega}$ = vorticity curl $\vec{V}$

Introduction

Vortex flows are among the most difficult to analyze because of their inherently nonlinear interactions. One therefore tries to study a model problem that contains only one generic aspect of such flows in a simple setting, free of other complications, in order to reach a better understanding. But it is not easy to find a simple two-dimensional model problem of vortex flow, preferrably with an analytic solution, because many of these are often time dependent and even unstable. One inviscid model, however, of steady flow past a slender conical delta wing of infinite length in which a vortex is shed from the leading edge has been studied numerically and has offered insight into the nature of the problem (see the two recent reviews[1,2] and the references therein). The vortex in reality is formed by the rolling up of the shed shear layer. In the limit of the vanishing viscosity of the model the shear layer shrinks in thickness to a vortex sheet, which coils up into a spiral having an infinite number of turns. Actually a vortex core never forms at the center of this theoretical inviscid spiral, and hence is unrealistic in terms of detailed core structure which is a viscous phenomena. In practical computations at most only a few turns of the coil are accurately resolved before the structure of the spiral is either lost in the dissipation inherent in a finite representation, or is replaced by another model for the core, e.g. a line vortex. In either case an accurate and detailed representation of the core structure is doubtful. But just outside the core the model does represent accurately the global quantities like circulation around the core. And the vortex sheet is the appropriate model to study the dynamics and stability of the rollup process since its inflexional velocity profile suggests that an instability would be inviscid in nature. Although one might expect a Rayleigh instability, Moore[3,4], making the two-dimensional time-dependent analogy, has analyzed the problem of the coiling sheet and found it to be marginally stable to 2D disturbances, the shortest wave-lengths being the least stable. The stretching of the sheet as it winds tighter into the spiral is the stabilizing process. In addition computational models have been formulated for the corresponding 3D problem where the wing is given a trailing edge and so truncated to a finite length. If the flow is subsonic, it cannot be strictly conical. The upwash at the trailing edge then produces a 3D

* Aerodynamics Department and Royal Institute of Technology, Stockholm
+ Principal Consultant

disturbance that makes the flow locally nonconical, but a number of numerical computations[5-8] indicate that the resulting sheet structure still remains stable even in equally high resolution simulations as the one we present here, although a recent result may indicate a splitting of the core vorticity[9]. Evidently the disturbance is not great enough to upset stability. Flows such as these, we believe, can be characterized as being of low helicity and hence are relatively stable.

The question we wish to raise here is: what happens to stability if the wing configuration is fundamentally nonconical and the flow is high speed and compressible? A good example of such a wing has a cranked delta planform, which is currently attracting considerable practical interest. In general the flowfield can be thought of as one with high helicity. At some angle of attack a vortex sheet is shed from the leading edge, but the precise dynamics of the sheet are not well understood. For example, is one single contiguous sheet shed along the entire leading edge, or do two distinct vortices form, and under what conditions the vortical features remain stable are still open questions.

In an earlier numerical investigation[10] of this wing in subsonic flow M_∞=0.3 but at the lower angle of attack α=10 deg., the vortex shed from the leading edge developed a spiralling mode in space but was steady in time. The computations agreed with the experiments reasonably well in board, and both indicated the loss of a coherent vortex outboard of the crank. We speculated that this unstable spiralling mode was the onset of a disordered vortex flow, and possibly the precursor of vortex bursting. In this paper we continue to explore this issue in the thrust of a numerical experiment offering high resolution in the mesh. The wing is the same but the incidence angle is higher in the hope of providing at least some preliminary insight on the nature of the spiralling mode and the behaviour of the computational model based on the Euler equations of motion. The results indicate that the sheet remains intact after undergoing the disturbance of the crank but it does not wrap around into a double-branched spiral. Instead the disturbance creates waves on the sheet which grow streamwise and tend to break up the sheet near the trailing edge. The increase in the overall lift on the wing in going from 10 deg., to 12.5 deg. incidence suggests that only a small fraction of the energy in the coherent vortex structure is being drained off to support the chaotic features. But because the flow still possesses substantial lift, we do not believe the vortical structure has broken down completely in the usual sense. At 12.5 deg, however, the flow is not steady. At 20 deg. incidence the computed flow is steady but a very significant part of the energy of the coherent vortex has been drained off, and the vortex appears to have burst.

Vorticity and Flow Instability

The concept of a cranked delta wing is a hybrid one. The design goal is to achieve the qualities of the low-aspect-ratio wing, high isobar sweep across midspan and vortex lift at high speed, and to improve the tip-stalling behaviour at low speeds. Since cranked delta wings have been studied mostly at low speeds, our discussion begins for the case of incompressible flow. At some angle of attack a vortex sheet is shed from the leading edge. Figure 1 outlines three possible scenarios for the dynamics of that sheet. The wing is sketched with a side edge at the tip which gives rise to a tip vortex, but our discussion is concerned mainly with what happens at the crank in the leading edge. The model Hoeijmakers[11] uses to study this configuration assumes that at the crank the sheet remains intact but the change in sweep angle sets up a disturbance that causes the sheet to coil up into a double-branched spiral (Fig. 1a). In the scenario of Brennenstuhl and Hummel[12], based on wind tunnel observations, the sheet tears at the crank (Fig. 1b) and leaves a section inboard whose two free edges spiral up to form an inboard vortex which is not fed beyond the crank. The section outboard, if a sheet is shed at all, also rolls up into the outboard vortex. In both scenarios two distinct vortices of like sign are created and rotate about one another. The flow structure is taken to be stable and composed only of large-scale motions. As the angle of attack increases the co-rotating vortices have been observed to merge before reaching the trailing edge. At still higher angles of attack the occurence of vortex breakdown was reported[12]. This then leads to the third scenario (Fig. 1c) that suggests that the tearing process may bring about an instability in the sheet, which is a precursor to complete breakdown. Two vortices still form here, but the sheet shreds at the crank, and together with the two cores, they all disintegrate into a less-ordered, but standing-wave pattern, of vortical structures. Helicity would be high. The details of this scenario are still one of conjecture, for there is not yet any clear-cut experimental evidence to tell us anything else with more certainty.

The basis for belief in the likelihood of the last scenario being correct rests on the inviscid instability of the vortical motion. Let us sketch how this might come about by analogy to simpler situations. Consider first the simple case of an isolated vortex filament in an inviscid and incompressible fluid. A varying curva-

ture immediately induces a torsion. The coupling of these two phenomena, curvature and torsion, was studied by Betchov[13] for the case of a plane vortex filament of variable curvature. The different segments of the filament move out of the plane at different induced velocities, and thus it acquires torsion. In general, if a curve moves under the influence of its own segments, two equations can be constructed specifying the evolution of the radius of curvature and of the torsion. Betchov studied these equations for the case of a helicoidal filament and found that it moves in space with a translation velocity and a rotation producing a tangential velocity. He found two opposing mechanisms in the system of equations, one an intensification of the torsion and the other a dispersion of the torsion, but the analysis indicates that the filament may find a statistical equilibrium between the two. He speculated that it might be one step on the way to the onset of chaotic motion.

This process describes a way that a single filament may undergo growth and diminishment simultaneously but still achieve a balanced state in equilibrium. Snow[14] has found that a three- dimensional disturbance can set off an instability in a vortical flow with a highly sheared azimuthal velocity component. Both of these cases at least suggest the possibility of a mechanism to transfer energy from large-scale to small-scale motion, the so- called energy cascade.

Everything we have said so far pertains to low-speed incompressible flow. Even less is known about the compressible situation, including what takes place at breakdown[15,16]. But the strong demand for practical knowledge about this case motivates us to explore it numerically. To begin the discussion, the dynamics now are governed by the vorticity equation for compressible nonisentropic flow with velocity $\vec{V}$

$$\frac{D}{Dt}\frac{\vec{\omega}}{\rho} = \frac{\vec{\omega}}{\rho}\cdot\varepsilon + \frac{1}{\rho^3}(\text{grad } \rho \times \text{grad } p) \qquad (1)$$

where $\vec{\omega}$= curl $\vec{V}$ and ε is the rate-of-strain tensor ;

$$\varepsilon = \frac{1}{2}(\text{grad } \vec{V} + \text{grad}^T \vec{V})$$

At transonic speed we can expect the vorticity to be amplified by variations in density, through non-isentropic processes like shock waves (the second term on the right), and by stretching in a straining velocity field (the first term on the right). The inboard vortex creates a straining velocity, but since the vorticity is nearly parallel to the velocity, the stretching term is rather small, and so also is the helicity. The vorticity in the shear layer, however, must follow the leading edge, so at the crank it takes a new direction and it seems likely that the stretching term will be large in this region. For the same reason the helicity, defined as $\vec{V}\cdot\vec{\omega}$, may reach a local maximum. We may find, therefore, an intensification of vorticity taking place in the vicinity of the crank. Once that happens it becomes a hopelessly complex situation to come to grips with, and the dynamics of vorticity can only be foretold by a numerical solution of the governing equations.

Motivated by the practical interest in this case, the aim of this paper is to carry out an exploratory numerical computation based on the Euler equations for compressible flow around a cranked delta wing in order to reach at least a preliminary understanding of the dynamics of the vortex features. By these simulations, using even the highest numerical resolution possible, we cannot, however, hope to answer all the outstanding questions surrounding this problem. Our goal is more in the spirit of tracing a broad outline of the phenomena involved, along with offering some elementary explanations for their presence, as a means to establish a suitable phenomenological model. This may help to guide the way to more fruitful analysis in the future.

Numerical-Simulation Procedure

Let us first look more closely at two alternative computational models for inviscid incompressible vortex flow. Hoeijmakers[5] has devised a method based upon a panel technique that inserts a vortex sheet into the solution as a discontinuity and adjusts it to be compatible with the surrounding potential field, usually termed vortex-sheet fitting. The strong point of this approach is the absence of diffusion of the sheet, while its limitation is that the overall starting location and topology of the sheet must be specified before hand. An alternative is to solve the incompressible Euler equations numerically on a grid. The vortex sheet, smeared out over a number of mesh cells, then is obtained automatically as part of the numerical solution, usually termed vortex-sheet capturing[7]. Its weakness is that all the flow features must be supported by the mesh, and this implies a certain amount of dissipation that varies with the spacing of the mesh. Thus a vortex sheet diffuses over a number of cells. On the other hand the strong point of this approach is that no information about the topology of the sheet needs to be specified prior to the solution. The smeared sheet can meander exactly as it likes, provided there are sufficient grid points to maintain its general structure. A recent comparison of results from these two methods for incompressible flow past a conical delta wing of finite length shows remarkable agreement in the position and strength of the vortical features[17]. It demonstrates that even with a mesh of less than 80 000 cells the diffusion has not brought about any substantial deterioration in the overall accuracy of the results.

Since all flow features naturally diffuse in any numerical simulation, they are sharpest when resolved with the highest possible density of mesh points allowed by the size of current super-computer memories. Therefore we have used Eriksson's method of transfinite interpolation[18] to construct a boundary-conforming O-O type mesh with just over 600 000 cells around the cranked delta wing (Fig. 2), the finest mesh that we can work with at this time. The mesh spacing shown here sets the scale of the shortest modes resolvable in the flow.

The Euler equations for compressible flow can be expressed as an integral balance of the conservation laws

$$\frac{\partial}{\partial t}\iiint q \, dvol + \iint \underline{H}(q)\cdot\underline{n} \, ds = \iint T \, ds \quad (2)$$

where q is the vector with elements of mass and momentum. Since the total enthalpy in the steady flow under consideration here is constant, the energy equation is not needed in the system. The inviscid flux quantity $\underline{H}(q)\cdot\underline{n}$ represents the net flux of q transported across, plus the pressure p acting on, the surface S surrounding the volume of fluid. The term T is the artificial viscosity model. It has the property of an energy sink for the shortest modes, i.e. $(d/dt)q^2<0$ summed over all the cells including those at the boundaries. Thus the method is dissipative. The finite-volume scheme then discretizes (2) by assuming that q is a cell-averaged quantity located in the center of the cell, and the flux term $\underline{H}(q)\cdot\underline{n}$ is defined only at the cell faces by averaging the values on each side. With these definitions and calling the cell surfaces in the three cooordinate directions of the mesh $\underline{S}_I$, $\underline{S}_J$, and $\underline{S}_K$, we obtain the finite volume form for cell ijk

$$\frac{\partial}{\partial t}q_{ijk}+\left[\delta_I(\underline{H}\cdot\underline{S}_I)+\delta_J(\underline{H}\cdot\underline{S}_J)+\delta_K(\underline{H}\cdot\underline{S}_K)\right]_{ijk}=$$

$$=(\delta_I+\delta_J+\delta_K)T \quad (3)$$

where $\delta_I(\underline{H}\cdot\underline{S}_I)\cong(\underline{H}\cdot\underline{S}_I)_{i+1/2}-(\underline{H}\cdot\underline{S}_I)_{i-1/2}$ is the centered difference operator. A more detailed description of the method is given in Ref. 19. With the appropriate boundary conditions we integrate this last equation with the two-level three-stage scheme

$$\begin{aligned} q_o &:= q^n \\ q' &:= q_o + \Delta t\ FD(q_o) \\ q'' &:= q_o + \Delta t\left[1/2\ FD(q_o) + 1/2\ FD(q')\right] \\ q^{n+1} &:= q_o + \Delta t\left[1/2\ FD(q_o) + 1/2\ FD(q'')\right] \end{aligned}$$

that steps the solution forward in time. Because a local time step Δt is used, true time accuracy is not obtained. But when a steady state exists, the procedure is capable to reach it, and when one does not exist, the pseudo-time iterations do not converge. The method has been under development for a number of years. It is well-tested, and in an extensive series of comparisons with other methods it has proven to be accurate and reliable[20].

Data Structure and Methodology for Vector Processing

The nature of the vector instructions in current supercomputers emphasizes rapid operations upon contiguous cells in memory. A three-dimensional structure suitable for vector processing is correctly visualized as consisting of a collection of adjacent pencils of memory cells with suitable boundary conditions. In conjunction with the data-structure design, key features of the vector processing procedure are: 1) separate storage arrays are assigned for the dependent variables q, flux component F, and flux differences FD, 2) one extra unit is dimensioned for each computational direction to hold the boundary conditions, and 3) flux differences are taken throughout the entire field by off-setting the starting location of the flux vector F. In this way all of the work in updating interior points is exclusively vector operations without any data motion. The vector lengths obtained are long, containing about 50,000 elements, and span 3D subsets of the data. This high degree of vectorization allows processing very large data sets most effectively.

Simulated Vortex Flowfield

The flow model (2) and (3) that we have described dissipates phenomena whose wavelength is on the order of the mesh spacing. The smaller we make the mesh spacing by adding more grid points, the finer the scale-length of the phenomena that we can resolve without it being obliterated by the dissipation. In this way the simulation procedure acts as a low-pass filter on the features we observe where the cut-off wave-length is set by the fineness of the mesh (Fig. 3). The usual mesh dimensions, say about 80,000 cells, can support only the large-scale features, which we presume are stable. But what happens if we use a much finer mesh? Smaller scale features, if they are present, will then be represented in the numerical solution. And it is just these short waves that Moore's stability analysis[3,4] suggests are the most unstable.

We have hypothesized that, given a sufficient number of grid points to resolve the shed shear layer and limit its diffusion, the numerical solution of the Euler equations does provide useful information about the dynamics of the free shear layer around the cranked delta wing[10]. In particular if the resolution is sharp enough, one may determine whether the shed sheet is stable, as in scenarios 1 and 2, or unstable, as in scenario 3. Furthermore, we have conjectured that if the sheet is unstable to short-wave perturbations, small-scale motions will be generated and supported by energy transferred from the large-scale motion[10]. If so the model will reflect the inertial range in the energy spectrum sketched in

Fig. 3. In our model the transfer of energy must be a steady process, similar at least in this regard to the one discussed by Betchov.

If this line of attack on the problem is to succeed, we must be able to refine the mesh sufficiently so that the resolved spectrum reaches far enough into the small scales in order to capture the suspected unstable modes. If it does not, we will never see the instability. The recent construction of a CYBER 205 supercomputer with 16 M words of real memory just now allows the use of more dense meshes than what was possible before. Of course there will always be those modes that are smaller than the resolution of our mesh, no matter how big our computer is. And we can say nothing about these modes. All we can do is construct several meshes of varying mesh fineness, and then compare the solutions computed upon them in order to establish the trend as the resolution increases, as we have done in Ref. 10.

Results of Numerical Experiment

The structures in the flowfields are surveyed by contour plots of the flow properties, primarily normalized static pressure $1-p/p_{t\infty}$ to identify shock waves and expansion regions, and total pressure coefficient $1-p_t/p_{t\infty}$ to show the shear layers and the shocks. By comparing these two sets of contours together, one can differentiate the shear layers from the shocks. Selected views of contours of Mach number are presented also. The two solution are obtained on the same mesh having the identical number of cells in each of the coordinate dimensions (160×48×80).

The contour lines on the wing surface in both cases indicate that a dramatic change in the footprint of the vortex takes place in the vicinity of the leading edge crank. The change is one from ordered vortex flow inboard of the crank to disordered flow outboard which is due, we believe, to the spiralling motion brought about by the torsional forces in a curving vortex filament. We saw this same feature at 10 deg. incidence also[10,21]. All three results suggest the third scenario where the vortex sheet shed form the leading edge tears at the crank and then develops unstable high-spatial-frequency modes. At 10 deg. incidence these modes are stable, i.e. they are standing waves and do not change with time. We also found that these high-frequency modes are fed by a relatively small drain of energy from the large-scale coherent vortex flow. This situation changes at the two higher incidence angles we investigate here.

a) Incidence α=12.5 deg.

For conditions M_∞=0.3 α=12.5 deg. Fig. 4 presents contour lines of the flow on the upper surface of the wing and in a mesh surface intersecting the wing along a constant local chord station. The contours reveal a strong and ordered vortex from the apex up to the crank where it is dispersed and becomes disordered. The lift and drag computed for this case C_L=0.634, C_D=0.124, compare well with those measured in a wind tunnel experiment[22] C_L=0.66, C_D=0.14. This good agreement, however, is misleading because after 1500 time iterations the computed solution is not steady. During the last 300 iterations the lift coefficient oscillates above and below the level of 0.65 by as much as 30%. The designers of this wing have reported that the measurements also suggest unsteady flow. It would appear then that unlike the case at 10 deg. incidence, this case is one of unstable modes oscillating in both space and time.

b) Incidence α = 20 deg.

Figure 5 surveys the flow computed for M_∞=0.3 α=20 deg. in the same way as Fig. 4. The footprint here also breaks up at the crank, but now the pressure trough is not as deep as in Fig. 4, so the ordered vortex inboard of the crank is not as strong. This corresponds to a substantial loss in lift. The coefficents for this computed case are C_L=0.516 and C_D=0.182 , and they are very steady. In contrast to the previous case, convergence was reached in 500 time iterations and lift and drag were absolutely steady during the last 100 iterations. These observations might suggest that at 10 deg. incidence unstable modes are present but steady and drain only a small fraction of the energy in the coherent flow, at 12.5 deg. these modes become unsteady, and at 20 deg. they drain off so much energy that the vortex has burst and the flow becomes steady again. The experiment, however, contradicts the conclusion of vortex bursting because the measured lift and drag are much higher C_L=0.88 C_D=0.32. Although there may be reasons for these great differences, the experimental model included the fuselage for example, which may be shedding nose vortices that somehow stabilize the flow, one must conclude that the computer simulation falsely predicts vortex bursting in this case.

A further comparsion with experiment provides additional insight. Figure 6 contains the chordwise comparison at 4 span locations of the surface pressures computed in the fine mesh with those measured in the wind tunnel[22]. (Because it is so thin, the tip section of the model contains only upper-surface taps.) The physical model includes a fuselage, but the numerical one does not. On the lower surface the agreement of all results is quite good. On the upper surface the inboard sections at y/b=0.25 and 0.50 show good agreement for the position and strength of the vortex as evidenced by the suction peaks it produces. The agreement in the next two sections is considerably worse, however. Near the crank at y/b=0.75 a discernible vortex suction peak is found

but it is weaker and broader and somewhat downstream of the measured one. In the tip section y/b=0.9 there are no peaks in either the computed or the measured values, and this suggests the absence of acoherent vortex. Quantitatively, however, both sets of computed pressures differ from the measured values by as much as a factor of two at the leading edge. Possible explanations for this discrepancy may be the influence of the fuselage of the model, including the shedding of nose vortices, and aeroelastic effects at the tip of the model. It seems more likely, however, that the flow in these two sections are undergoing a complex transition from a coherent leading- edge vortex inboard to a disordered vortex flow at the tip, and it is difficult to model this situation. For flows at low angle of attack the model also has produced results in good agreement with a panel method[21].

Figure 7 displays the way lift varies with angle of attack α in our computations presented here and previously[10,21] and compares it with that measured experimentally. The numerical simulation appears to predict vortex bursting prematurely.

Final Remarks

Vortical flows are among the most baffling for the fluid dynamicist to understand. They are susceptible to instabilities, they can develop local regions of extreme velocity and vorticity, and they are inherently nonlinear. So they are prime subjects for numerical study. Here one aspect of vortical flow, the behaviour of the leading edge vortex over a cranked delta wing at high incidence has been studied. With sufficient degrees of freedom given to the solution by the mesh size, small-scale torsional-wave effects due to the cranked leading edge have been observed in the flowfield. At 12.5 deg. incidence high lift is still maintained, and both the experiments and the computations indicate that the vortex has not burst. The flow, however, is unstady. Wind tunnel measurements verify that the results of the numerical simulation bears a certain amount of realism. At the highest incidence α=20 deg., the computer simulation indicates that the flow is steady but the leading edge vortex has burst. The experiments, however, show a stronger vortex that has not burst.

Acknowledgements

The authors thank Mr. P. Sacher of MBB-Ottobrunn for suggesting that we study this flow around the TKF wing, and Mr. G. Cucinelli of MBB-Ottobrunn for his assistance in evaluating the results and comparing them with the experiments. The computer time provided by the Control Data Corporation to carry out these computations on its large-memory CYBER 205 is gratefully acknowledged.

References

1 Hoeijmakers, H.W.M: Numerical Computation of Vortical Flows About Wings, NLR Report MP 83073 U, Amsterdam, 1983.

2 Smith, J.H.B.: Theoretical Modelling of Three-Dimensional Vortex Flows in Aerodynamics. Aero J., April 1984, pp. 101-116.

3 Moore, D.W., and Griffith-Jones, R: The Stability of an Expanding Circular Vortex Sheet, Mathematika, Vol. 21, 1974, pp. 128-133.

4 Moore, D.W.: The Stability of an Evolving Two-Dimensional Vortex Sheet, Mathematika, Vol. 23, 1976, pp.35-44.

5 Hoeijmakers, H.W.M and Vaatstra, W.: A Higher-Order Panel Method Applied to Vortex Sheet Roll-Up. AIAA J. Vol. 21, No. 4, 1983, pp. 516-523.

6 Krause, E., Shi, X.G., and Hartwich, P.M.: Computation of Leading-Edge Vortices, AIAA Paper 83-1907, 1983.

7 Rizzi, A., and Eriksson, L.E.: Computation of Inviscid Incompressible Flow with Rotation, J. Fluid Mech, Vol. 153, 1985, pp. 275-312.

8 Rizzi, A.: Euler Solutions of Transonic Vortex Flows Around the Dillner Wing. J. Aircraft, Vol. 22. April 1985, pp. 325-328.

9 Rizzi, A.: Multi-Cell Vortices Observed in Fine-Mesh Solutions to the Incompressible Euler Equations, in Super Computers and Fluid Dynamics, ed. K. Kuwahara, Lect. Notes Engineering, Springer, to appear.

10 Rizzi, A., and Purcell, C.J.: Numerical Experiment with Inviscid Vortex Stretched Flow Around a Cranked Delta Wing: Subsonic Speed, AIAA Paper No. 85-4080, 1985.

11 Hoeijmakers, H.W.M., Waatstra, W. and Verhaagen, N.G.: On the Vortex Flow over Delta and Double-Delta Wings. J. Aircraft. Vol. 20, No. 9, 1983, pp. 825-832.

12 Brennenstuhl, U., and Hummel, D.: Vortex Formation Over Double-Delta-Wings, ICAS Paper, 82-6.6.3, 1982.

13 Betchov, R.: On the Curvature and Torsion of an Isolated Vortex Filament, J. Fluid Mech., Vol. 22, 1965, pp. 471-479.

14 Snow, J.T.: On Inertial Instability as Related to the Multiple-Vortex Phenomenon. J. Atmos Sci, Vol. 35, Sept 1978, pp. 1660-1677.

15 Hall, M.G.: Vortex Breakdown, Ann Rev Fluid Mech, Vol. 4, 1972, pp. 195-218.

16 Leibovich, S.: The Structure of Vortex Breakdown, Ann Rev Fluid Mech, Vol. 10, 1978, pp. 221-246.

17 Hoeijmakers, H.W.M., and Rizzi, A.: Vortex-Fitted Potential Solution Compared with Vortex-Captured Euler Solution for Delta Wing with Leading Edge Vortex Separation. AIAA Paper 84-2144, 1984.

18 Eriksson, L.E.: Generation of Boundary-Conforming Grids around Wing-Body Configurations using Transfinite Interpolation, AIAA J., Vol. 20, Oct. 1982, pp. 1313-1320.

19 Rizzi, A.W. and Eriksson, L.E.: Computation of Flow Around Wings Based on the Euler Equations, J. Fluid Mech, Vol. 148, Nov. 1984, pp. 45-71.

20 Smith, J.H.B.: Numerical Solutions for Three-Dimensional Cases - Delta Wings, in Test Cases for Inviscid Flow Field Methods. AGARD AR-211, Paris, 1985.

21 Fornasier, L., and Rizzi, A.: Comparisons of Results from a Panel Method and an Euler Code for a Cranked Delta Wing, AIAA Paper No. 85-4091, 1985.

22 Le Fauga, A.: Untersuchungen des elastischen Verhaltens eines sogenannten starren Windkanalmodells, MBB Report, LKE 294 – ACA-R24, Munich, 1982.

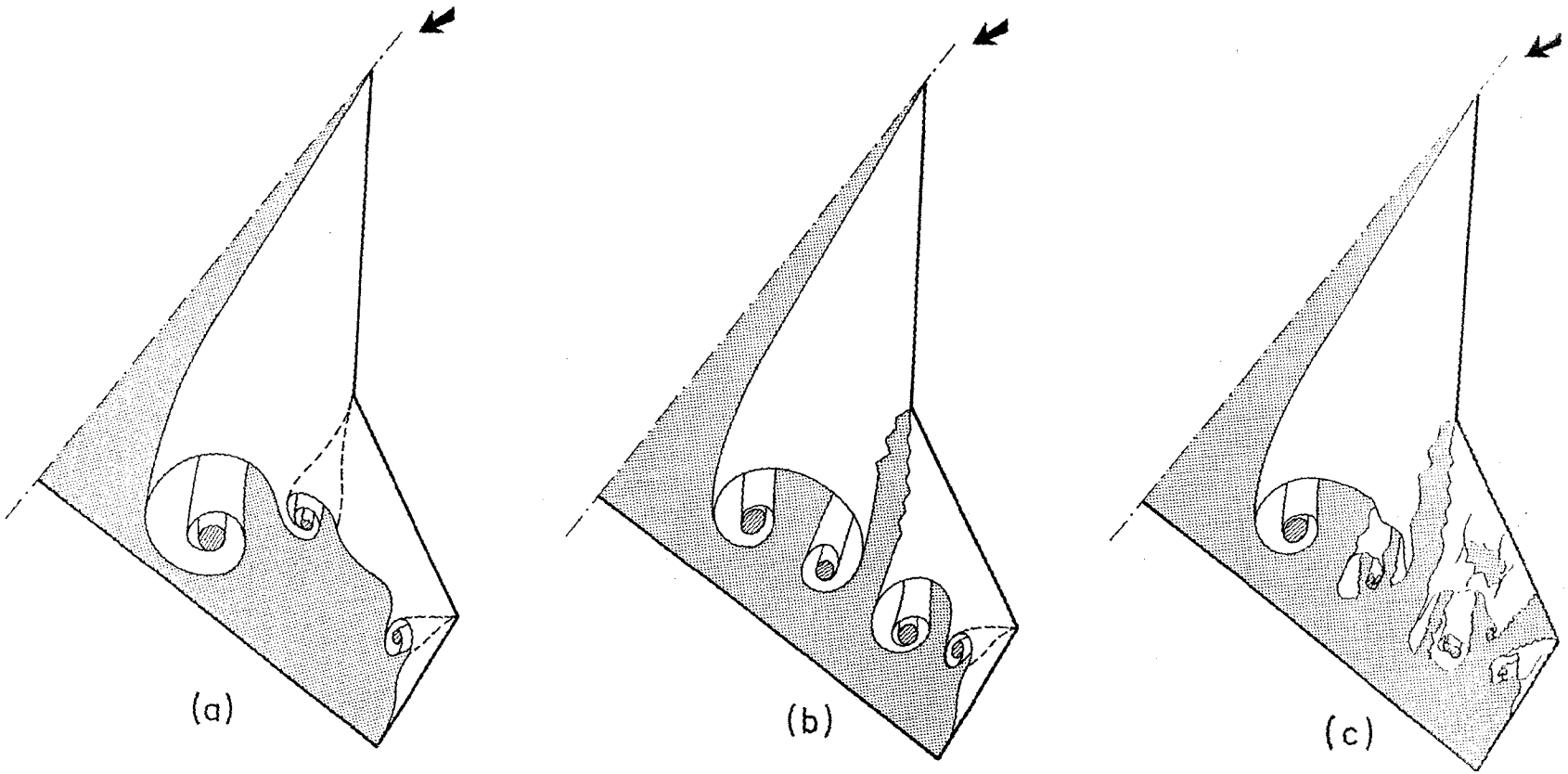

Fig. 1 Three scenarios for the dynamics of the shed sheet: a) intact sheet with double-branched spiral, b) sheet tears but is stable, c) sheet tears and in unstable.

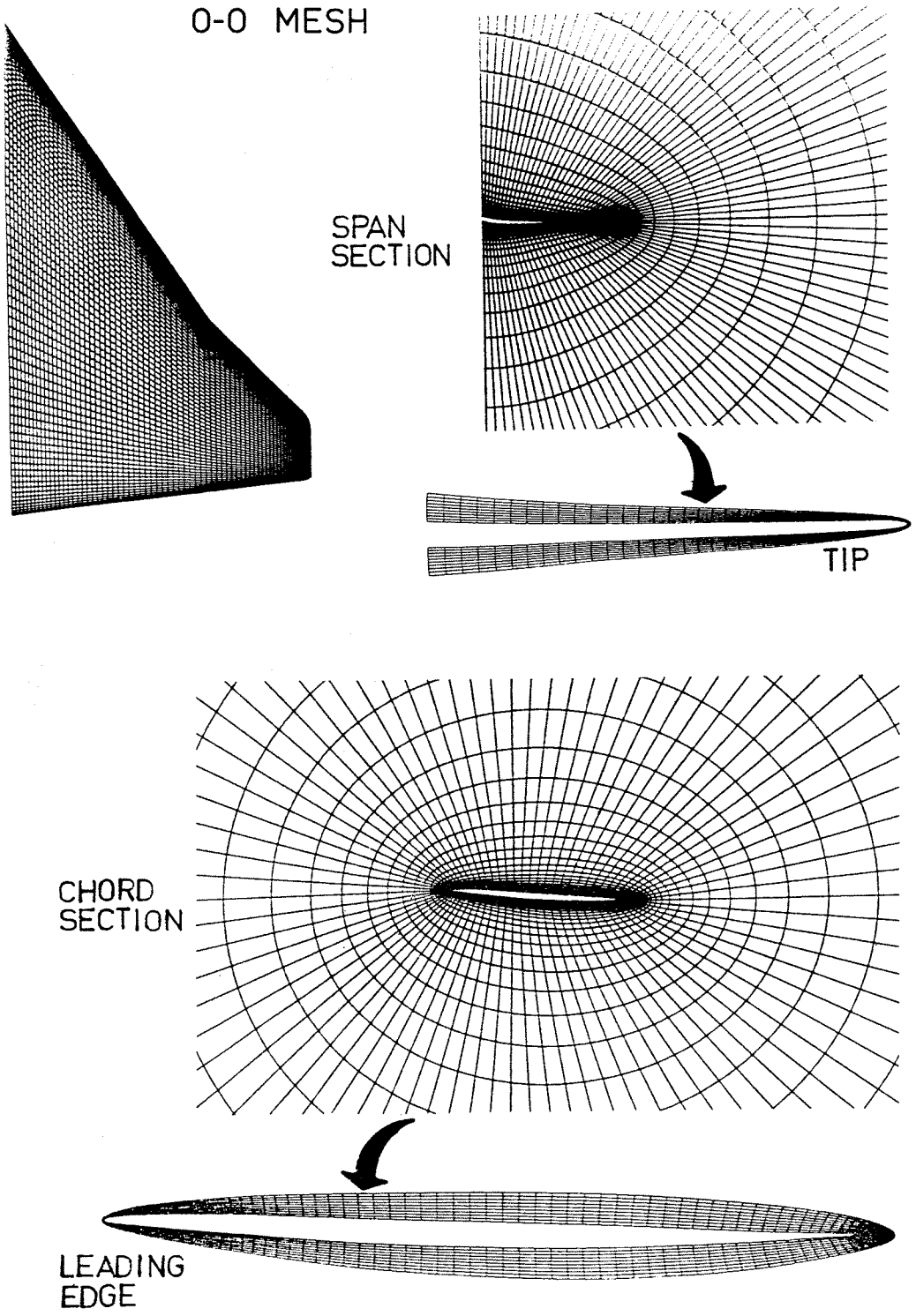

Fig. 2a) O-O type mesh with 160 × 48 × 80 cells around a cranked delta wing.

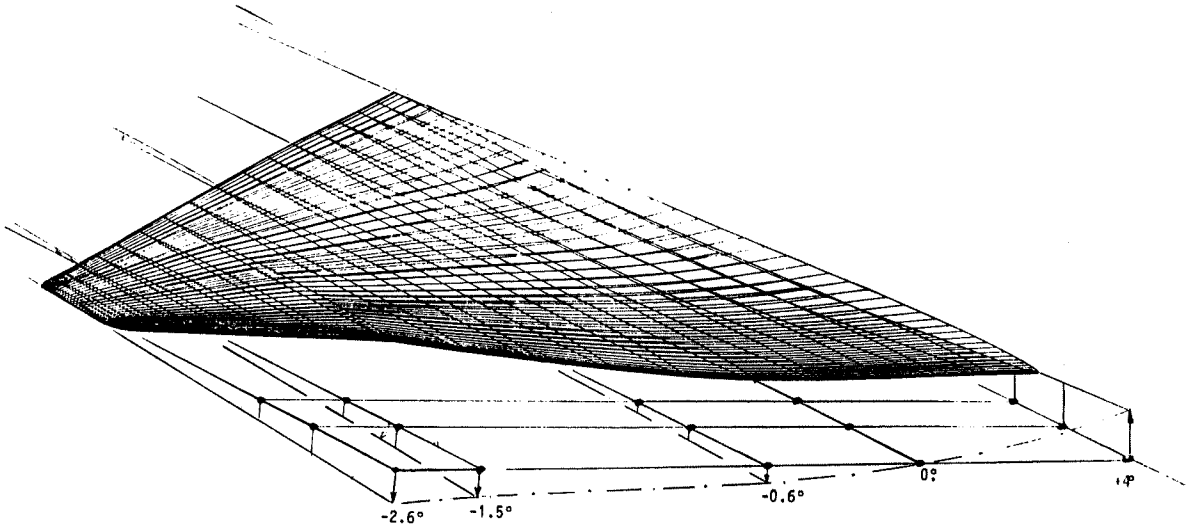

Fig. 2b) Twist angles of cranked delta.

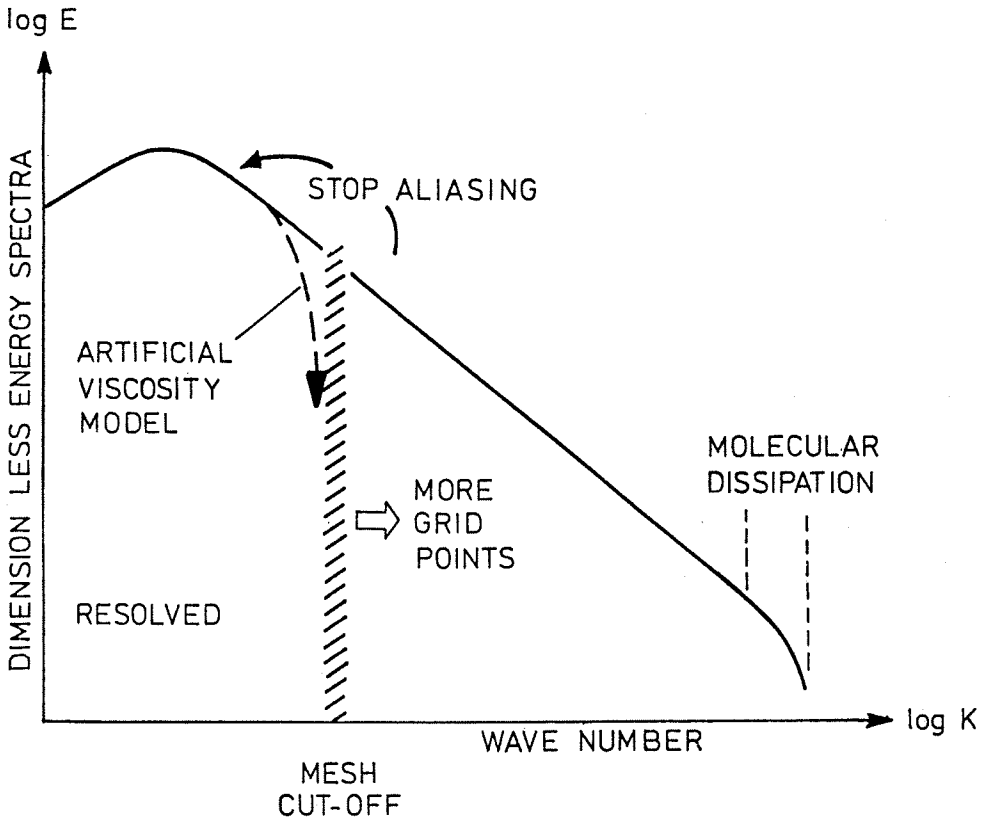

Fig. 3 The numerical method acts as a low-pass filter on the solution. The more points added to the mesh, the higher the wave number resolved.

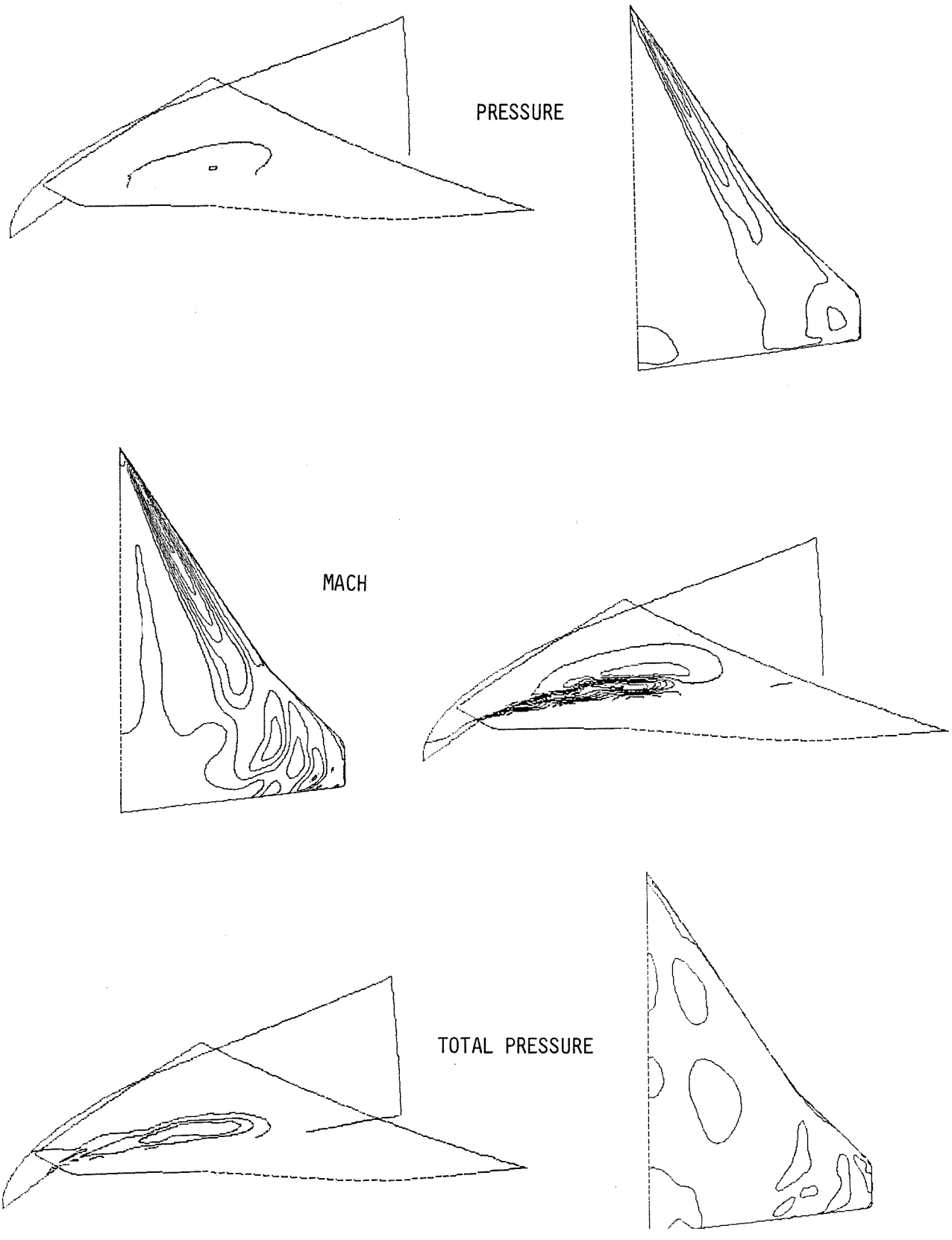

Fig. 4 Flowfield computed with fine mesh of $160 \times 48 \times 80$ cells. $M_\infty = 0.3$, $\alpha = 12.5$ deg. Contours of normalized pressure $1-p/p_{t_\infty}$, Mach number, and total pressure $1-p_t/p_{t_\infty}$. Over wing and upper surface.

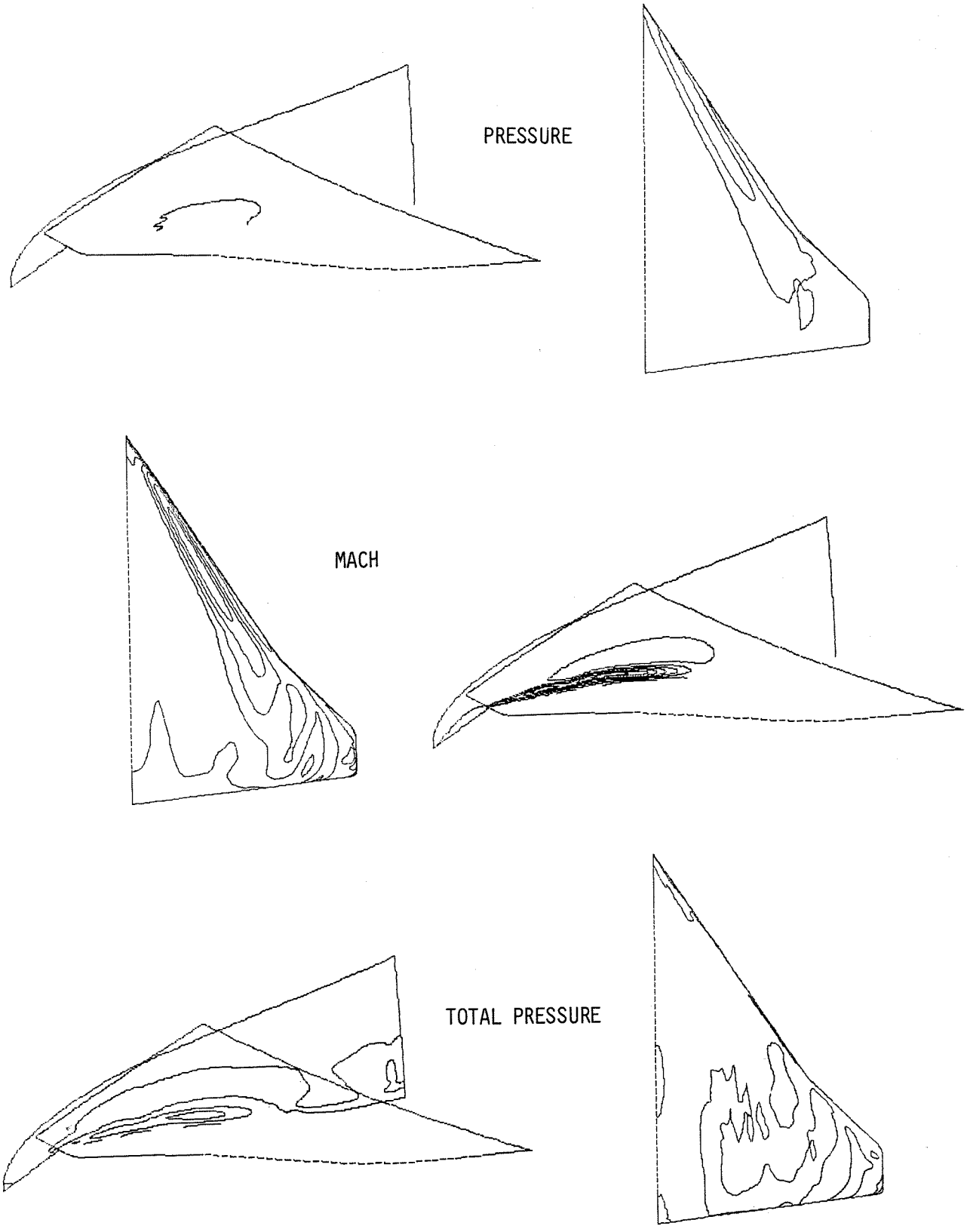

Fig. 5 Flowfield computed with fine mech of $160 \times 48 \times 80$ cells. $M_\infty = 0.3$, $\alpha = 20$ deg. Contours of normallized pressure $1-p/p_{t_\infty}$, Mach number, and total pressure $1-p_t/p_{t_\infty}$. Over wing and on upper surface.

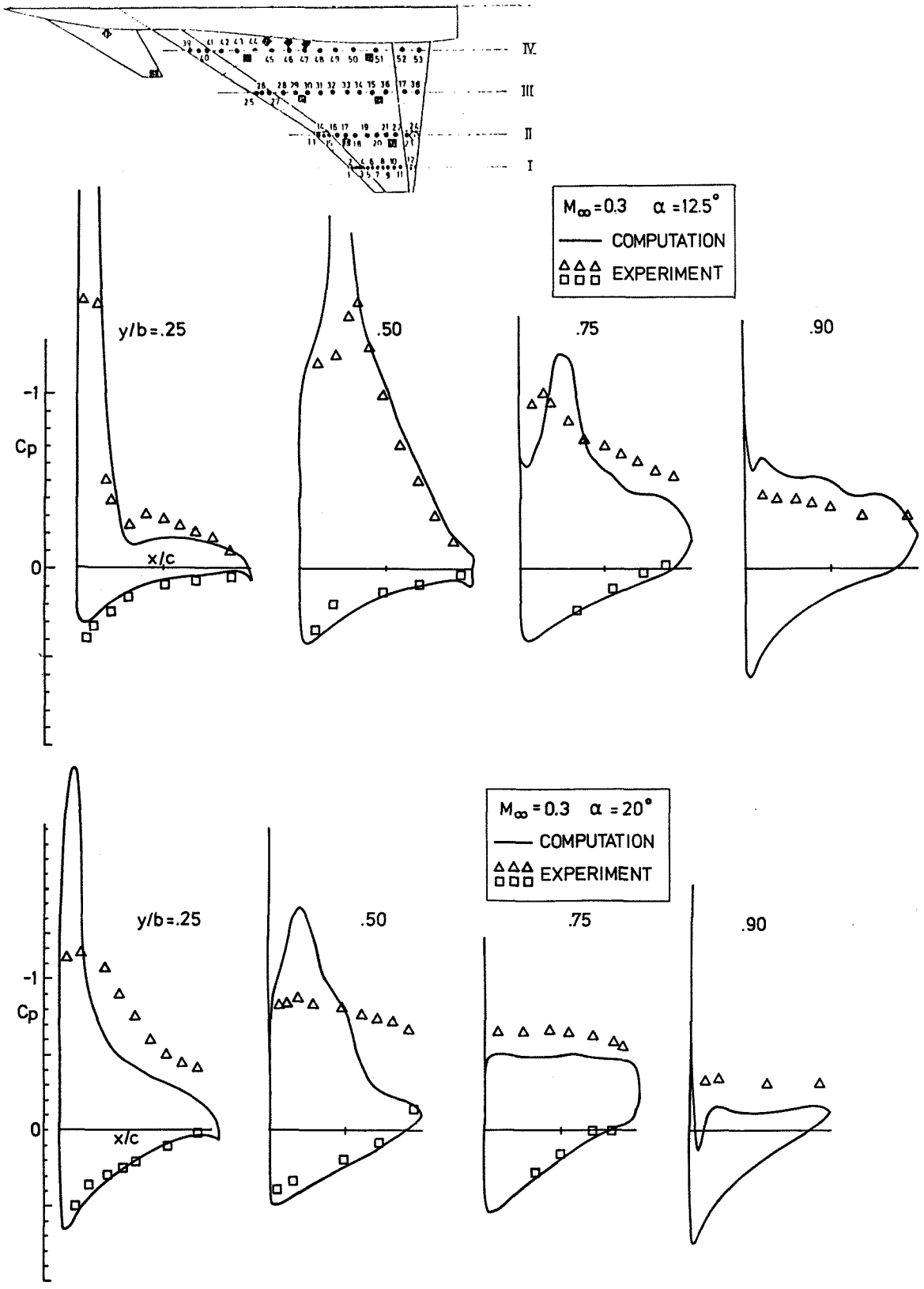

Fig. 6 Surface pressure coefficients C_p computed with the fine mesh and compared with wind tunnel measurements along chordwise sections.

a) $M_\infty = 0.3$, $\alpha = 12.5$ deg.

b) $M_\infty = 0.3$, $\alpha = 20$ deg

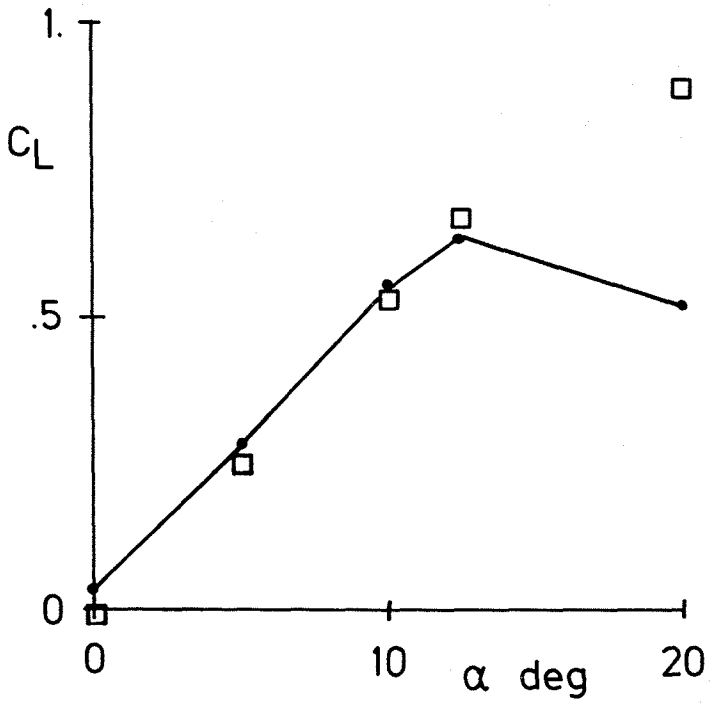

Fig. 7 Variation of lift C_L with angle of attack (see also Ref. 10 and 21).